HHS Public Access

Author manuscript

Clin Cancer Res. Author manuscript; available in PMC 2017 July 06.

Published in final edited form as:

Clin Cancer Res. 2016 February 15; 22(4): 923–934. doi:10.1158/1078-0432.CCR-15-0187.

Cabozantinib (XL184) Inhibits Growth and Invasion of Preclinical TNBC Models

Mansoureh Sameni[1], **Elizabeth A. Tovar**[2], **Curt J. Essenburg**[2], **Anita Chalasani**[1], **Erik S. Linklater**[2], **Andrew Borgman**[3], **David M. Cherba**[3], **Arulselvi Anbalagan**[1], **Mary E. Winn**[3], **Carrie R. Graveel**[2], and **Bonnie F. Sloane**[1,4]

[1]Department of Pharmacology, Wayne State University School of Medicine, Detroit, Michigan

[2]Center for Cancer and Cell Biology, Van Andel Research Institute, Grand Rapids, Michigan

[3]Bioinformatics and Biostatistics Core, Van Andel Research Institute, Grand Rapids, Michigan

[4]Karmanos Cancer Institute, Wayne State University, Detroit, Michigan

Abstract

Purpose—Triple-negative breast cancer (TNBC) is an aggressive breast cancer subtype that is associated with poor clinical outcome. There is a vital need for effective targeted therapeutics for TNBC patients, yet treatment strategies are challenged by the significant intertumoral heterogeneity within the TNBC subtype and its surrounding microenvironment. Receptor tyrosine kinases (RTK) are highly expressed in several TNBC subtypes and are promising therapeutic targets. In this study, we targeted the MET receptor, which is highly expressed across several TNBC subtypes.

Experimental Design—Using the small-molecule inhibitor cabozantinib (XL184), we examined the efficacy of MET inhibition in preclinical models that recapitulate human TNBC and its microenvironment. To analyze the dynamic interactions between TNBC cells and fibroblasts over time, we utilized a 3D model referred to as MAME (Mammary Architecture and Microenvironment Engineering) with quantitative image analysis. To investigate cabozantinib

Corresponding Author: Carrie R. Graveel, Center for Cancer and Cell Biology, Van Andel Research Institute, 333 Bostwick Avenue, Grand Rapids, MI 49503. Phone: 616-234-5788; Fax: 616-234-5789; carrie.graveel@vai.org.
C.R. Graveel and B.F. Sloane contributed equally to this article.

Note: Supplementary data for this article are available at Clinical Cancer Research Online (http://clincancerres.aacrjournals.org/).

Disclosure of Potential Conflicts of Interest

C.R. Graveel reports receiving commercial research grants from Mirati Therapeutics. No potential conflicts of interest were disclosed by the other authors.

Authors' Contributions

Conception and design: C.R. Graveel, B.F. Sloane
Development of methodology: M. Sameni, E.A. Tovar, A. Chalasani, A. Anbalagan
Acquisition of data (provided animals, acquired and managed patients, provided facilities, etc.): M. Sameni, E.A. Tovar, C.J. Essenburg, A. Chalasani, E.S. Linklater
Analysis and interpretation of data (e.g., statistical analysis, biostatistics, computational analysis): M. Sameni, A. Borgman, D.M. Cherba, M.E. Winn, C.R. Graveel, B.F. Sloane
Writing, review, and/or revision of the manuscript: M. Sameni, E.S. Linklater, M.E. Winn, C.R. Graveel, B.F. Sloane
Administrative, technical, or material support (i.e., reporting or organizing data, constructing databases): A. Borgman, A. Anbalagan, M.E. Winn
Study supervision: C.R. Graveel, B.F. Sloane

inhibition *in vivo*, we used a novel xenograft model that expresses human HGF and supports paracrine MET signaling.

Results—XL184 treatment of MAME cultures of MDA-MB-231 and HCC70 cells (± HGF-expressing fibroblasts) was cytotoxic and significantly reduced multicellular invasive outgrowths, even in cultures with HGF-expressing fibroblasts. Treatment with XL184 had no significant effects on MET^{neg} breast cancer cell growth. *In vivo* assays demonstrated that cabozantinib treatment significantly inhibited TNBC growth and metastasis.

Conclusions—Using preclinical TNBC models that recapitulate the breast tumor microenvironment, we demonstrate that cabozantinib inhibition is an effective therapeutic strategy in several TNBC subtypes.

Introduction

Triple-negative breast cancer (TNBC) accounts for 15% to 20% of breast cancers and is associated with advanced stage at diagnosis and poorer outcome compared with other breast cancer subtypes (1). TNBC is characterized by the lack of estrogen receptor (ER) and progesterone receptor (PR) expression and HER2 receptor amplification. Characteristic clinical features of TNBC include a peak in recurrence risk within the first 3 years, a peak of cancer-related death in the first 5 years, and a weak relationship between the tumor size and lymph node metastasis (2). At the molecular level, TNBC has significant overlap with the basal-like subtype with approximately 80% of TNBCs being classified as basal-like (1). Recent studies involving comprehensive gene expression analysis of TNBC cases revealed extensive molecular heterogeneity within TNBC and identified four to six distinct molecular TNBC subtypes (3, 4). These subtypes have unique expression signatures and ontologies and are defined as basal-like, mesenchymal, and luminal androgen receptor subtypes.

There is an urgent need for effective targeted therapeutics for TNBC patients; however, new treatment strategies are challenged by the significant intertumoral heterogeneity of TNBCs. Currently, TNBCs are treated with cytotoxic combination chemotherapy, with platinum-based therapies having the highest response rates. Only 22% of TNBC patients have a complete response to neoadjuvant chemotherapy (5) and therefore require additional therapeutic approaches. Receptor tyrosine kinases (RTK) and growth factors are highly expressed in several TNBC subtypes (3) and are attractive therapeutic targets. The success of trastuzumab in $HER2^{+}$ breast cancer underscores the promise of targeting tyrosine kinases, yet several tyrosine kinase inhibitors (TKI) have had only limited success in the clinic due to diverse mechanisms of resistance. In breast cancer and most other cancers, multiple RTKs are frequently activated and contribute to resistance by providing functional redundancy of critical signaling networks (6, 7). Another component of breast cancer that has been revealed to play a significant role in progression and therapeutic resistance is the tumor microenvironment (TME; refs. 8–10). Despite the overwhelming data on the influence of the TME, cancer therapeutics are directed primarily at the tumor cells. The design of successful TNBC treatment strategies will need to take into consideration both the intertumoral heterogeneity of TNBCs and the signaling pathways that promote both progression and resistance.

The RTK MET drives several oncogenic processes, including invasion, proliferation, and survival, and is involved in the progression and metastasis of most solid human cancers (11). In breast cancer, MET is overexpressed in 20% to 30% of cases and is a strong, independent predictor of poor clinical outcome (12–16). We previously demonstrated that MET is expressed in all molecular subtypes of breast cancer, but we observe the highest expression in basal-like (TNBC) breast cancers (17, 18). These findings have been supported by several other studies on MET in basal-like breast cancers [for review, see (19, 20)]. Recently, we demonstrated that MET is coexpressed in the majority of $HER2^+$ breast cancers and may be involved in therapeutic resistance to HER2-targeted therapies (21). These findings demonstrate that MET overexpression commonly occurs in the more aggressive breast cancer subtypes (i.e., TNBC) and may be a novel therapeutic target. In cancer, aberrant MET signaling can occur through overexpression of MET or HGF, amplification, mutation, or autocrine signaling. MET signaling is also frequently elevated in tumors due to increased secretion of HGF by cancer-associated fibroblasts (CAF). The exact mechanism by which MET signaling is dysregulated in TNBC has not been elucidated.

The TME is composed of a complex network of stromal cells, immune cells, extracellular matrix, and cytokines/chemokines that is also influenced by pH and hypoxia. The paracrine interactions between the tumor epithelium and TME have been shown to be critical for the invasive, metastatic, and resistant tumor phenotypes. A recent study found that cocultures with CAFs induce HGF signaling in basal-like, but not luminal-like breast cancer cells (22). We have shown that mammary fibroblasts engineered to secrete high levels of HGF (MF:HGF) enhance proteolysis and invasiveness of a preinvasive TNBC cell line (MCF10.DCIS) in 3D cocultures and progression to invasive carcinomas *in vivo* (8). These studies underscore the influence of the TME on RTK signaling and breast cancer progression.

In this study, we examined the efficacy of MET inhibition on TNBC progression *in vitro* and *in vivo*. We utilized the small-molecule inhibitor cabozantinib (XL184), which potently inhibits MET and VEGFR2 (23). Clinical activity with cabozantinib has been demonstrated in a range of cancers. A striking clinical result of cabozantinib is the significant decrease in bone metastases seen on bone scans in castrate-resistant prostate cancer patients (24, 25). Cabozantinib is being tested in a phase II clinical trial for metastatic TNBC and phase III clinical trials for metastatic renal carcinoma and hepatocellular carcinoma and has been FDA approved for treatment of metastatic medullary thyroid cancer. To analyze the temporal and dynamic interactions between the epithelial tumor cells and CAFs, we employed a 3D model referred to as MAME (Mammary Architecture and Microenvironment Engineering) and quantitative image analysis. We have previously shown that MAME cocultures are able to recapitulate tumor-TME interactions, the invasive phenotype that occurs *in vivo*, and model the ability of antagonists to reduce invasion (8, 26, 27; Sameni and Sloane, unpublished). For investigation of MET inhibition *in vivo*, we utilized a novel xenograft model that expresses human HGF on an immunocompromised SCID background. Because mouse HGF binds human MET with low affinity (28), traditional immunocompromised mouse models do not effectively activate human MET signaling. The $hHGF^{tg}$-SCID model enhances the growth of MET-dependent human tumors, defines the HGF contribution to tumor growth, and is a valuable model for preclinical testing of inhibitors targeting the MET

signaling pathway (29, 30). Using these unique strategies, we are able to interrogate the efficacy of MET inhibition in environments in which both autocrine and paracrine signaling may be driving tumor progression.

Here, we observed that cabozantinib (XL184) inhibits growth and invasion of TNBC cells in both monocultures and cocultures with HGF-overexpressing fibroblasts or CAFs. This efficacy was observed for TNBC cell lines representing various TNBC molecular subtypes. Even though cabozantinib inhibits kinase activity of MET and VEGFR2, cabozantinib was ineffective against MET^{neg} TNBC cells. These findings imply that MET signaling is a crucial signaling node in TNBC growth and invasion. Additional *in vivo* studies demonstrated that cabozantinib treatment was highly effective in inhibiting TNBC progression and metastasis. In summary, these results reveal that cabozantinib inhibition may be a highly effective treatment strategy for TNBC patients.

Materials and Methods

Antibodies and reagents

Cabozantinib (XL184) was kindly provided by Exelixis. Reconstituted basement membrane (rBM; Cultrex) was purchased from Trevigen. Alexa Fluor 546 phalloidin, DAPI, Slow Fade Reagent, FITC-conjugated affinity-purified donkey anti-rabbit IgG and normal donkey serum, Click-it^{R}EDU assay, Live/Dead Viability/Cytotoxicity Kits and Leibovitz L15 medium were from Life Technologies. Ki67 antibody was from Abcam. Cignal Lenti-RFP was purchased from Qiagen and Lenti-YFP from Lentigen. Protease/phosphatase inhibitor cocktail (#5872) was purchased from Cell Signaling Technology. Mammary epithelial basal medium (MEBM) without phenol red and MEGM was purchased from Lonza. Fetal bovine serum (FBS) was from HyClone. Bovine serum albumin, antibiotics, Triton X-100 and all other chemicals, unless otherwise stated, were purchased from Sigma. See Immunoblot Analysis and Experimental Lung Metastasis for additional antibodies.

Cell lines

All cell lines were cultured in basal medium supplemented with 10% fetal calf serum (MDA-MB-231, DMEM; MDA-MB-468, Liebovitz L-15 media; HCC70, DMEM; and Hs578T, DMEM + 10 μg/mL bovine insulin). Cells were originally purchased from American Type Culture Collection (ATCC). The WS12Ti fibroblasts are a human breast carcinoma associated fibroblast cell line that was isolated at Karmanos Cancer Institute (31, 32). MF:HGF is a normal human breast fibroblast line that has been engineered to express GFP and secrete high levels of HGF (a kind gift of Dr. Kuperwasser, Tufts University Boston, MA; ref. 33). MDA-MB-231 and HCC70 were transduced with Cignal Lenti-RFP and WS12Ti with Lenti-YFP in order to distinguish among the cell types in 3D cocultures. Cell lines were authenticated using the STR PowerPlex 16 system (Promega).

MAME cultures of TNBC cells ± MF:HGF or CAFs

MDA-MB-231 and HCC70 cells were grown as monocultures or in cocultures with CAF or MF:HGF cells. Details for establishing and analyzing MAME cultures are described in detail in Results and Supplementary Data (34).

Immunofluorescent staining

HCC70 and MDA-MB-231 cells were grown on glass coverslips to 40% to 50% confluency in triplicate. Media were changed to serum-free MEGM 24 hours prior to treatment. Cells were treated with DMSO or 2 μmol/L XL184 or vehicle (DMSO) for 25 minutes at 37°C. Then 100 ng/mL HGF (R&D Systems) was added to the cells in the presence or absence of XL184 and incubated at 37°C for 5 minutes. Cells were fixed with 4% formaldehyde in PBS for 15 minutes at room temperature (RT), followed by washing in PBS, and then incubated in blocking buffer (5% normal donkey serum/0.3% Triton X-100 in PBS) for 1 hour at RT. The cells were incubated with primary antibody, phospho-Met (Tyr1234/Tyr1235)(D26) XP Rabbit mAb (Cell Signaling Technology, 1:50), overnight at 4°C, and then incubated with Alexa Fluor 488-conjugated secondary antibody (Life Technologies) to enable fluorescent detection for 2 hours at RT. Nuclei were labeled with DAPI and cells were mounted with Slowfade gold antifade reagent (Invitrogen). Images were visualized on a Zeiss LSM 780 confocal microscope.

Immunoblot analysis

Whole-cell lysates were collected in a RIPA buffer containing protease/phosphatase inhibitor cocktail (Cell Signaling Technology). HCC70, MDA-MB-231, MDA-MB-468, Hs578T, CAFs, and MF:HGF were grown for 6 days, treated with 2 μmol/L of XL184 for 30 minutes, washed with PBS containing protease/phosphatase inhibitor cocktail and harvested in RIPA buffer plus inhibitor cocktail. For blots shown in Supplementary Figs. S1 and S2, cells were treated with HGF and/or XL184 for 24 hours. For 3D cultures, the cells were grown for 6 days in rBM-coated dishes, treated as above, washed with sterile PBS containing protease/phosphatase inhibitor cocktail, scraped in cold PBS 5 mmol/L EDTA plus inhibitor cocktail, placed on ice, washed 2 times for 1 hour each to remove rBM, and then RIPA buffer containing inhibitor cocktail was added to the cell pellets. Lysates were loaded based on DNA concentrations.

Lysates (20–40 μg) were resolved on a 4% to 20% TGX SDS-PAGE gel (Bio-Rad) and transferred to a PVDF membrane (Invitrogen). After blocking for 1 hour with 5% dry milk in TBST buffer (20 mmol/L Tris-HCl pH 7.4, 150 mmol/L NaCl, 0.1% Tween-20), blots were probed overnight at 4°C with the following primary antibodies from Cell Signaling Technology: Met (DC12), pMET (Y1234/Y1235; D26), AKT (#9272), pAKT (S473; #9271), MAPK (#9102), pMAPK (Thr202/Tyr204; #9101), and β-tubulin (#2146). Blots were reacted with peroxidase-conjugated antibody for 1 hour, followed by visualization of the proteins using ECL detection reagents (Amersham).

Live/Dead viability/cytotoxicity assay

MDA-MB-231 alone or together with MF:HGF or Ws12Ti cells were seeded on rBM with 2% rBM overlay. Vehicle control or 2 μmol/L XL184 were added at day 0 and replaced every other day. At day 6 or 12, the Live/Dead assay was performed as previously described (35).

In vivo efficacy studies

All animal studies were conducted with protocols approved by the Institutional Animal Care and Use Committee of the Van Andel Research Institute. The breeding and genotyping of the hHGF^{tg}-SCID mice has been previously described (29). Female mice ages 4 to 8 weeks were used for the tumor growth kinetic experiments. Age-matched C3H-SCID littermates from the same mating cages as the hHGF^{tg}-SCID mice were used as experimental controls. For orthotopic tumor formation, subconfluent cells were harvested and resuspended in serum-free DMEM or RPMI at concentrations of 1×10^6 cells/mL. Each animal received 100 μL of cell suspension injected s.c. into the mammary fat pad. Tumor-bearing mice for each mouse strain (either hHGF^{tg}-SCID or C3H-SCID) were randomized into two groups (10 mice/group) for treatment with vehicle or XL184 (30 mg/kg, once daily). Following cell injection, mice were monitored for tumor formation twice weekly and tumor volume was measured with manual calipers [volume (mm^3) = length × width × depth]. Treatment started when the average tumor size reached 150 mm^3 and drugs were administered for 21 days. For the established tumor study, only hHGF^{tg}-SCID animals were used and treatment started when the average tumor size reached 500 mm^3. Linear mixed-effects models were used to test for significant differences in drug response across treatment arms; the XenoCat modeling framework (36) was leveraged to increase statistical power for poorly growing xenograft.

Experimental lung metastasis assay

For lung metastasis formation, 5.0×10^5 MDA-MB-231 cells were washed and harvested in HBSS and subsequently injected into the lateral tail vein in a volume of 0.2 mL. Mice were treated with vehicle or XL184 (30 mg/kg, once daily) starting the following day. Endpoint assays were conducted at 14 days after injection unless significant morbidity required that the mouse be euthanized earlier. Pulmonary metastases were identified both by perfusing with 15% India ink solution and bleaching the collected lungs in Fekete's solution. For quantitation, fixed sections were cut every 200 μm and immunostained for human MHC Class I alpha antibody (EP1395Y; Abcam). Stained sections were scanned on the Aperio XT ScanScope and lung metastases were quantitated using multispectral image analysis. Positive pixel percentage was determined by quantitating the percentage of pixels positive for human MHC Class I alpha staining per total tissue area in each section.

Results

Effect of XL184 on MET signaling in TNBC and fibroblast cells

To understand how XL184 treatment affects MET signaling, we first examined MET expression and activity in multiple TNBC cell lines that are representative of several TNBC subtypes identified by Lehmann and colleagues (3). These cell lines correspond to the two major basal-like subtypes and a mesenchymal-like subtype that were identified by the Pietenpol laboratory. This included Hs578t (mesenchymal stem-like; basal B), MDA-MB-231 (mesenchymal stem-like; basal B), MDA-MB-468 (basal-like 1; basal A), and HCC-70 (basal-like 2, basal A) cells. We observed high MET expression in Hs578t and HCC-70 cells, moderate expression in MDA-MB-231 cells, and low expression in MDA-MB-468 cells (Fig. 1A). In 2D cultures, we observed MET phosphorylation (pMET) in

HCC70 cells, which expressed the highest levels of MET. MET activation was inhibited with XL184 treatment (Fig. 1A); however, MET phosphorylation was unaffected by MEK inhibition via U0126 (Fig. 1D). To confirm that MET phosphorylation was inhibited by XL184, we treated HCC70 cells with HGF and examined MET Y1234/1235 and Y1349 phosphorylation (Supplementary Fig. S1A and S1B). Both pMET Y1234/1235 and pMET Y1349 were activated by exogenous HGF and inhibited by XL184 even in the presence of HGF. We also examined MET activation and inhibition in HCC70 and MDA-MB-231 cells using immunofluorescence (Fig. 1B; Supplementary Fig. S1D). Here we observed low basal levels of pMet Y1234/Y1235 in vehicle-treated HCC70 cells (Fig. 1B, top left). Treatment with HGF induced increased pMET levels and membrane localization (Fig. 1B, bottom left). Upon XL184 treatment, there was a significant decrease in pMET and membrane localization in both HGF- and non-HGF–treated cells (Fig. 1B, right). A similar pattern was observed in MDA-MB-231 cells, yet membrane localization was stronger in HCC70 cells (Supplementary Fig. S1D). We also examined MET expression and activation in two fibroblast lines that were utilized in the 3D coculture experiments (Fig. 1A, right). The normal breast fibroblast line MF:HGF exhibited very weak MET expression, whereas the CAF line WS12Ti expressed moderate levels of MET. HGF expression was observed to be slightly higher in the MF:HGF fibroblasts than in the WS12Ti CAFs (Supplementary Fig. S1C). Even though HGF is not expressed in normal epithelial cells, low to moderate expression was observed in TNBC cells (Supplementary Fig. S1C).

The PI3K/AKT and MAPK/ERK pathways are critical mediators for maintaining proliferative and invasive signaling during RTK activation. It is hypothesized that signaling plasticity among RTKs is necessary for maintaining PI3K/AKT and MAPK/ERK signaling during tumor progression. MET strongly activates both the PI3K/AKT and MAPK pathways and these signaling effectors may reflect MET inhibition and signaling mechanisms of resistance. We evaluated the effect of XL184 treatment on these pathways and observed only a small decrease in AKT phosphorylation and an increase in total AKT expression in MDA-MB-231 and Hs578t cells (Fig. 1C). The opposite effect was observed with MEK inhibition where AKT phosphorylation increased in the presence of U1026 in both MDA-MB-231 and HCC70 cells (Fig. 1E). Interestingly, we observed a significant decrease in pAKT and an increase in total AKT in both the MF:HGF and WS12Ti fibroblast cells in the presence of XL184 (Fig. 1C). For the MAPK pathway, we observed a moderate increase in pMAPK in XL184-treated HCC70 and MDA-MB-468 cells (Fig. 1C). Again, the opposite affect was observed in the fibroblast lines, where both MF:HGF and WS12Ti cells had a decrease in MAPK activity when treated with XL184. In comparing MET inhibition to MEK inhibition, we observed that U0126 treatment caused a significant decrease in MAPK activation (Fig. 1E). In 3D monocultures of MDA-MB-231 and HCC70 cells, we observed similar MAPK signaling changes with XL184 treatment (Fig. 1F). In the MDA-MB-231 cells, there was no change in pMAPK with MET inhibition, whereas in HCC70 cells MET inhibition led to an increase of pMAPK activity. No change in total MET was detected with XL184 treatment. We also evaluated the effect of MET inhibition on ERK5 expression and activity (Supplementary Fig. S2). We observed a minimal increase in total ERK5 expression in MDA-MB-231 cells treated with XL184, yet did not see any significant changes in pERK5 in HCC70 or MDA-MB-231 cells. Overall, we observed distinct effects of MET and MEK

inhibition in TNBC cells. These results also revealed a divergent response to MET inhibition in TNBC cells versus fibroblasts.

XL184 abrogates TNBC growth in MAME cultures

To recapitulate the architecture of invasive carcinomas and their associated signaling networks, we utilized 3D MAME coculture models and performed live-cell imaging in real-time to examine responses to XL184 treatment. The MAME cocultures are a tractable system based on the 3D reconstituted basement membrane culture models used by the Bissell and Brugge laboratories [for review, see (37, 38)]. Our MAME models allow for coculture of multiple cell types in the context of a 3D microenvironment and have been optimized for live-cell imaging of real-time interactions among the cells (34). Because MDA-MB-231 and HCC70 cell lines represent two different TNBC subtypes, are highly invasive *in vitro*, and are capable of developing tumors *in vivo*, these lines were used in the following assays. We first examined the effects of XL184 treatment on the TNBC cells grown in 3D reconstituted basement membrane overlay cultures using protocols we have described (39). For cocultures, MF:HGF or WS12Ti CAF cells were seeded in addition to TNBC cells. Cellular structures were allowed to develop for 4 days before the addition of XL184, which was replaced every 2 days with structures being imaged on day 10 (Fig. 2A). In monocultures of MDA-MB-231 and HCC70 cells, we observed significant dose–response reductions in volume of the multicellular 3D structures with XL184 treatment (Fig. 2B and E). Even though we saw greater inhibition at 4 to 6 μmol/L, the drug had a tendency to precipitate in 3D cultures at these higher concentrations (dosing ranges were based on studies in Yakes and colleagues; ref. 23). For this reason, subsequent experiments were performed with 2 μmol/L XL184. Next, we examined the effect of XL184 treatment on TNBC growth both alone and in coculture with MF:HGF cells. XL184 caused a significant decrease in volume and a reduction in the number of structures formed by MDA-MB-231 cells grown either alone or in coculture with MF:HGF cells (Fig. 2C and D). XL184 similarly reduced the volume and number of structures formed by HCC70 cells grown either alone or in coculture with MF:HGF cells (Fig. 2F and G). We also evaluated the effect of MEK inhibition on MDA-MB-231 growth (Supplementary Fig. S3). Even though MEK inhibition reduced MDA-MB-231 volume, we observed a greater reduction in structure volume with XL184 treatment. This suggests that while targeting downstream effectors of the MET signaling pathway may be effective in TNBC, greater efficacy is observed by targeting the MET receptor. These observations parallel the results we observed with the selective MET inhibitor SU11274 in MAME cocultures of triple-negative DCIS cell lines and MF:HGF fibroblasts (8).

XL184 has no effect on invasion or volume of MET^{neg} TNBC cells

XL184 is known to have activity against MET and VEGFR2. To verify that the efficacy of XL184 on TNBC growth is mediated through the MET pathway, we examined the effect of XL184 on both MET^{pos} (MDA-MB-231 and HCC70) and MET^{neg} (T47D) cell lines in coculture with MF:HGF cells. T47D is a luminal breast cancer cell line that is commonly used as a negative control for MET expression. XL184 treatment reduced invasive outgrowths and significantly decreased the volume of structures formed by MET^{pos} and MF:HGF cells, but not invasive outgrowths or volume of the structures formed by MET^{neg}

(T47D) and MF:HGF cells (Fig. 3A and B). We also evaluated VEGF and VEGFR2 expression in the TNBC cells. Cytokine analysis revealed no VEGF expression and by Western blot analysis we observed minimal levels of VEGFR2 only in MDA-MB-231 cells (data not shown). These results verify that MET signaling is a vital pathway in the MET^{pos} TNBC cells that is abrogated with XL184 treatment.

XL184 treatment reduces multicellular invasive outgrowths from TNBC structures

As noted above, XL184 treatment appears to reduce the invasive phenotype of structures formed by MET^{pos} TNBC and HGF-over-expressing fibroblasts (see Fig. 3A). To further analyze possible effects of XL184 on the invasive phenotype, we used Volocity software to segment the 3D structures into cores (pseudocolored purple) and invasive outgrowths (pseudocolored green; Fig. 4A). A dramatic change in invasive outgrowths is illustrated by the reduced green fluorescence in structures treated with XL184 (Fig. 4B). Quantification of the volume of the structure cores and multicellular invasive outgrowths revealed that XL184 significantly reduced the volume of both cores and invasive outgrowths of MDA-MB-231 structures (Fig. 4C). XL184 also significantly reduced the volume of invasive outgrowths formed by MDA-MB-231 cells in coculture with MF:HGF cells, yet a significant decrease in core volume with XL184 treatment was not observed (Fig. 4D). These results suggest that HGF-expressing cells within the tumor microenvironment may reduce the efficacy of MET inhibitors against TNBC proliferation.

XL184 treatment is cytotoxic to TNBC monocultures and cocultures with fibroblasts

To further understand the effect of cabozantinib on TNBC proliferation we examined the effect of XL184 on live cells in TNBC monocultures or cocultures with fibroblasts. We observed that XL184 treatment reduced the number of live 3D structures (Fig. 5A) and volume of live structures (Fig. 5B) formed by MDA-MB-231 cells in monoculture and coculture with Ws12Ti cells (Fig. 5). A similar effect was observed in cocultures with MF:HGF cells (data not shown). Because tumor recovery after drug removal is a concerning clinical issue, we evaluated the persistence of XL184 treatment on growth suppression. In this experiment, cells were treated for 6 days with XL184 and then the drug was removed for 6 days before imaging (Supplementary Fig. S4). When treatment with XL184 was stopped, some recovery in growth was observed, consistent with XL184 inducing cytostasis in a subpopulation of the cells (40). XL184 does suppress proliferation as evidenced by a decrease in cells staining for the proliferation marker Ki67 in structures formed by MDA-MB-231 cells alone or in coculture with either CAFs or MF:HGF cells (data not shown).

XL184 is highly effective against TNBC tumor growth *in vivo*

To examine the efficacy of inhibiting MET *in vivo*, we injected MDA-MB-231 and HCC70 cells into the mammary fat pads of $hHGF^{tg}$-SCID and C3H-SCID animals. Because the $hHGF^{tg}$-SCID mice express human HGF, they are able to mimic the high HGF-expressing microenvironment of most cancers. When the tumors reached 150 mm^3, animals were treated with XL184 for 3 weeks. Both cell lines showed enhanced growth rates in the $hHGF^{tg}$-SCID mice (Fig. 6A) as compared with the C3H-SCID control mice (Supplementary Fig. S5A and S5B). MET inhibition with XL184 resulted in a significant decrease in tumor growth as compared with the vehicle ($P < 0.001$) for both MDA-MB-231

and HCC70 xenografts. Evaluation of MET activation in vehicle and XL184-treated tumors showed that MET is highly active in vehicle-treated tumors (Fig. 6B and D), whereas MET activity is only present in a thin layer of cells at the periphery in XL184-treated tumors (Fig. 6C and E). XL184 treatment caused significant necrosis in the majority of the tumor whereas the cells on the tumor periphery are proliferating (data not shown). These pMET positive cells at the tumor edge are surrounded by viable mammary fat pad and exposed to XL184 therefore it is likely that these cells represent a MET-positive resistant subpopulation. To examine the efficacy of XL184 against established TNBC growth, we started treatment after the MDA-MB-231 tumors were approximately 500 mm^3 (Fig. 6F). Even though XL184 significantly inhibited tumor growth ($P < 0.005$), the established tumors treated with XL184 have an upward growth trend likely due to resistance mechanisms being present in the late-stage tumors. The effect of MET inhibition on metastasis of MDA-MB-231 cells was determined in an experimental lung metastasis model. We observed that XL184 treatment significantly inhibited metastasis ($P < 0.02$) of TNBC cells to the lung (Fig. 6G). These *in vivo* studies validate our *in vitro* results and indicate that XL814 treatment is an effective therapeutic strategy for TNBC.

Discussion

TNBC comprises 15% to 20% of all breast cancers yet accounts for a disproportionate percentage of breast cancer deaths. This depressing statistic is largely attributable to the aggressive nature of the disease, its high molecular heterogeneity, and the lack of targeted therapies for TNBC (1, 2). Because TNBC often recurs within 3 to 5 years of diagnosis, there is a short timeframe in which to achieve a complete response in TNBC patients (2). The high expression of RTKs and growth factors across several TNBC subtypes makes targeting RTK signaling a promising therapeutic option for TNBC patients (3). In this study, we targeted the MET oncogene as it is a RTK that is highly expressed across several TNBC subtypes and numerous MET inhibitors are currently being tested in clinical trials.

The tumor microenvironment is a substantial component of a tumor that can significantly influence both breast cancer progression and treatment efficacy (41, 42). Nonetheless, the human breast cancer TME is often excluded in preclinical testing of targeted therapies. In this study, we used distinct *in vitro* and *in vivo* models that recapitulate the TNBC epithelium and TME. Our 3D MAME cocultures are able to model both progression to an invasive phenotype and the ability of antagonists to reduce that invasive phenotype. By employing MAME cultures of TNBC cell lines that represent different TNBC molecular subtypes in coculture with mammary fibroblasts and CAFS, we were able to test the efficacy of XL184 inhibition in a model that recapitulates the diverse tumor epithelium–stromal interactions of TNBC. This allowed us to evaluate the efficacy of cabozantinib against paracrine MET signaling as both the mammary fibroblasts and CAFs expressed high levels of HGF. We found that cabozantinib reduced the volume of 3D structures including their invasive outgrowths even in the presence of HGF-expressing CAFs.

The exploration of paracrine MET signaling was continued by *in vivo* analysis of MET inhibition through the use of the $hHGF^{tg}$-SCID model. Here we observed that MET^{pos} TNBC cells are significantly inhibited with cabozantinib. To model the treatment of

established human tumors, we delayed XL184 dosing until the tumors had reached 500 mm^3 (compared with 100 to 150 mm^3 in typical *in vivo* studies). Even though we observed a significant decrease in tumor growth, there is a clear upward growth trend that begins after the first week of treatment (Fig. 6F). This suggests that there may be therapeutic resistance to targeted MET inhibition in established or late-stage tumors. Resistance to TKI monotherapy is often observed in late-stage cancers. To avoid this therapeutic resistance it will be necessary to identify combination therapies that will target signaling nodes that are essential to tumor survival. One possibility is combination therapy of MET and MEK inhibitors. An increase in MAPK activity was observed in two TNBC cell lines after XL184 treatment (Fig. 1) and previously we observed increased MAPK activity in MET^{pos} cells treated with *MET* shRNA in $HER2^+$ breast cancers (21). MAPK activity may be increased in response to MET inhibition through several mechanisms, including activation of other RTKs (6, 7). Further studies are necessary to determine which receptors may be compensating for MET inhibition and if targeting MET and MEK in combination in TNBC is more effective.

Our findings and other studies suggest that MET inhibitors are most effective against high MET-expressing tumors (43, 44). Those studies focused on the primary tumor environment, yet MET may also be a critical therapeutic target in metastatic disease and chemotherapy-treated patients. Hypoxia and HIF1 expression are known to induce MET expression and activation of the downstream MET signaling cascades (45, 46). Because most primary and metastatic tumors contain hypoxic, avascular regions, MET inhibition also may be advantageous in combination with chemotherapy or in recurrent tumors that moderately express MET, but have high levels of hypoxia (47).

The present results are the first time that MET inhibition has been evaluated as a targeted therapeutic approach *in vitro* and *in vivo* in TNBC. Both our *in vitro* and *in vivo* preclinical models demonstrate that cabozantinib treatment is an effective therapeutic strategy in TNBC. Considering that TNBC is a highly heterogeneous disease, it is unlikely that a single targeted therapy will be effective for all TNBC patients. Therefore, it is critical that we develop multiple targeted therapeutic approaches in concert with diagnostic tests in order to identify TNBC patients who will benefit from specific therapeutic strategies. The necessity of companion diagnostics in the clinic has been underscored by the failure of TKIs in clinical trials, particularly MET inhibitors (48). These failures demonstrate that not only do we need clear diagnostic thresholds defined by receptor expression or activation, but we also need to understand the overall complexity of the kinase signaling networks. Because these signaling networks are heavily influenced by the TME, it is essential that preclinical studies utilize models, such as MAME, that can recapitulate this milieu. The combination of enhanced *in vitro* and *in vivo* models, companion diagnostics, and rationale clinical trial design will accelerate our development of successful targeted therapies.

Supplementary Material

Refer to Web version on PubMed Central for supplementary material.

Acknowledgments

The authors thank Lisa Turner for her excellence in histopathology and Bryn Eagleson, Sylvia Timmer, and the VARI Vivarium for their continuous dedication. The authors also thank Dafna Kaufman for her assistance with this study. Confocal microscopy was performed in the Microscopy, Imaging and Cytometry Resources Core of Wayne State University, which is supported by NIH Center grant P30 CA022453 to the Karmanos Cancer Institute, and the Perinatology Research Branch of the National Institutes of Child Health and Development. Cell line authentication was performed through the Biobanking and Correlative Sciences Core and the Applied Genomics Technology Center of Wayne State University, which are supported in part by NIH Center grant P30 CA022453 to the Karmanos Cancer Institute. The authors are also grateful to Dan DeSantis for his assistance with image processing.

Grant Support

This study was funded by the Department of Defense (DoD) W81XWH-11-1-0050 (B.F. Sloane and C.R. Graveel) and the Breast Cancer Research Foundation (C.R. Graveel).

References

1. Foulkes WD, Smith IE, Reis-Filho JS. Triple-negative breast cancer. N Engl J Med. 2010; 363:1938–48. [PubMed: 21067385]
2. Dent R, Trudeau M, Pritchard KI, Hanna WM, Kahn HK, Sawka CA, et al. Triple-negative breast cancer: clinical features and patterns of recurrence. Clin Cancer Res. 2007; 13:4429–34. [PubMed: 17671126]
3. Lehmann BD, Bauer JA, Chen X, Sanders ME, Chakravarthy AB, Shyr Y, et al. Identification of human triple-negative breast cancer subtypes and pre-clinical models for selection of targeted therapies. J Clin Invest. 2011; 121:2750–67. [PubMed: 21633166]
4. Burstein MD, Tsimelzon A, Poage GM, Covington KR, Contreras A, Fuqua SA, et al. Comprehensive genomic analysis identifies novel subtypes and targets of triple-negative breast cancer. Clin Cancer Res. 2015; 21:1688–98. [PubMed: 25208879]
5. Liedtke C, Mazouni C, Hess KR, Andre F, Tordai A, Mejia JA, et al. Response to neoadjuvant therapy and long-term survival in patients with triple-negative breast cancer. J Clin Oncol. 2008; 26:1275–81. [PubMed: 18250347]
6. Xu AM, Huang PH. Receptor tyrosine kinase coactivation networks in cancer. Cancer Res. 2010; 70:3857–60. [PubMed: 20406984]
7. Wilson TR, Fridlyand J, Yan Y, Penuel E, Burton L, Chan E, et al. Widespread potential for growth-factor-driven resistance to anticancer kinase inhibitors. Nature. 2012; 487:505–9. [PubMed: 22763448]
8. Jedeszko C, Victor BC, Podgorski I, Sloane BF. Fibroblast hepatocyte growth factor promotes invasion of human mammary ductal carcinoma in situ. Cancer Res. 2009; 69:9148–55. [PubMed: 19920187]
9. Tchou J, Conejo-Garcia J. Targeting the tumor stroma as a novel treatment strategy for breast cancer: shifting from the neoplastic cell-centric to a stroma-centric paradigm. Adv Pharmacol. 2012; 65:45–61. [PubMed: 22959023]
10. Rudnick JA, Kuperwasser C. Stromal biomarkers in breast cancer development and progression. Clin Exp Metastasis. 2012; 29:663–72. [PubMed: 22684404]
11. Birchmeier C, Birchmeier W, Gherardi E, Vande Woude GF. Met, metastasis, motility and more. Nat Rev Mol Cell Biol. 2003; 4:915–25. [PubMed: 14685170]
12. Ghoussoub RA, Dillon DA, D'Aquila T, Rimm EB, Fearon ER, Rimm DL. Expression of c-met is a strong independent prognostic factor in breast carcinoma. Cancer. 1998; 82:1513–20. [PubMed: 9554529]
13. Camp RL, Rimm EB, Rimm DL. Met expression is associated with poor outcome in patients with axillary lymph node negative breast carcinoma. Cancer. 1999; 86:2259–65. [PubMed: 10590366]
14. Ocal IT, Dollard-Filhart M, D'Aquila T, Camp RL, Rimm DL. Tissue microarray-based studies of patients with lymph node negative breast carcinoma show that met expression is associated with worse outcome but is not correlated with epidermal growth factor family receptors. Cancer. 2003; 97:1841–48. [PubMed: 12673709]

15. Edakuni G, Sasatomi E, Satoh T, Tokunaga O, Miyazaki K. Expression of the hepatocyte growth factor/c-Met pathway is increased at the cancer front in breast carcinoma. Pathol Int. 2001; 51:172–8. [PubMed: 11328532]
16. Lengyel E, Prechtel D, Resau JH, Gauger K, Welk A, Lindemann K, et al. C-Met overexpression in node-positive breast cancer identifies patients with poor clinical outcome independent of Her2/neu. Int J Cancer. 2005; 113:678–82. [PubMed: 15455388]
17. Graveel CR, DeGroot JD, Su Y, Koeman J, Dykema K, Leung S, et al. Met induces diverse mammary carcinomas in mice and is associated with human basal breast cancer. Proc Natl Acad Sci U S A. 2009; 106:12909–14. [PubMed: 19567831]
18. Ponzo MG, Lesurf R, Petkiewicz S, O'Malley FP, Pinnaduwage D, Andrulis IL, et al. Met induces mammary tumors with diverse histologies and is associated with poor outcome and human basal breast cancer. Proc Natl Acad Sci U S A. 2009; 106:12903–8. [PubMed: 19617568]
19. Ho-Yen CM, Green AR, Rakha EA, Brentnall AR, Ellis IO, Kermorgant S, et al. C-Met in invasive breast cancer: Is there a relationship with the basal-like subtype? Cancer. 2014; 120:163–71. [PubMed: 24150964]
20. Inanc M, Ozkan M, Karaca H, Berk V, Bozkurt O, Duran AO, et al. Cytokeratin 5/6, c-Met expressions, and PTEN loss prognostic indicators in triple-negative breast cancer. Med Oncol. 2014; 31:801. [PubMed: 24326984]
21. Paulson AK, Linklater ES, Berghuis BD, App CA, Oostendorp LD, Paulson JE, et al. MET and ERBB2 are coexpressed in ERBB2+ breast cancer and contribute to innate resistance. Mol Cancer Res. 2013; 11:1112–21. [PubMed: 23825050]
22. Camp JT, Elloumi F, Roman-Perez E, Rein J, Stewart DA, Harrell JC, et al. Interactions with fibroblasts are distinct in Basal-like and luminal breast cancers. Mol Cancer Res. 2011; 9:3–13. [PubMed: 21131600]
23. Yakes FM, Chen J, Tan J, Yamaguchi K, Shi Y, Yu P, et al. Cabozantinib (XL184), a novel MET and VEGFR2 inhibitor, simultaneously suppresses metastasis, angiogenesis, and tumor growth. Mol Cancer Ther. 2011; 10:2298–308. [PubMed: 21926191]
24. Lee RJ, Saylor PJ, Michaelson MD, Rothenberg SM, Smas ME, Miyamoto DT, et al. A dose-ranging study of cabozantinib in men with castration-resistant prostate cancer and bone metastases. Clin Cancer Res. 2013; 19:3088–94. [PubMed: 23553848]
25. Smith DC, Smith MR, Sweeney C, Elfiky AA, Logothetis C, Corn PG, et al. Cabozantinib in patients with advanced prostate cancer: results of a phase II randomized discontinuation trial. J Clin Oncol. 2013; 31:412–9. [PubMed: 23169517]
26. Bengsch F, Buck A, Gunther SC, Seiz JR, Tacke M, Pfeifer D, et al. Cell type-dependent pathogenic functions of overexpressed human cathepsin B in murine breast cancer progression. Oncogene. 2014; 33:4474–84. [PubMed: 24077280]
27. Moin K, Sameni M, Victor BC, Rothberg JM, Mattingly RR, Sloane BF. 3D/4D functional imaging of tumor-associated proteolysis: impact of microenvironment. Methods Enzymol. 2012; 506:175–94. [PubMed: 22341225]
28. Rong S, Bodescot M, Blair D, Dunn J, Nakamura T, Mizuno K, et al. Tumorigenicity of the *met* proto-oncogene and the gene for hepatocyte growth factor. Mol Cell Biol. 1992; 12:5152–8. [PubMed: 1406687]
29. Zhang YW, Su Y, Lanning N, Gustafson M, Shinomiya N, Zhao P, et al. Enhanced growth of human met-expressing xenografts in a new strain of immunocompromised mice transgenic for human hepatocyte growth factor/scatter factor. Oncogene. 2005; 24:101–6. [PubMed: 15531925]
30. Zhang YW, Staal B, Essenburg C, Su Y, Kang L, West R, et al. MET kinase inhibitor SGX523 synergizes with epidermal growth factor receptor inhibitor erlotinib in a hepatocyte growth factor-dependent fashion to suppress carcinoma growth. Cancer Res. 2010; 70:6880–90. [PubMed: 20643778]
31. Pauley RJ, Santner SJ, Tait LR, Bright RK, Santen RJ. Regulated CYP19 aromatase transcription in breast stromal fibroblasts. J Clin Endocrinol Metab. 2000; 85:837–46. [PubMed: 10690899]
32. Koblinski JE, Dosescu J, Sameni M, Moin K, Clark K, Sloane BF. Interaction of human breast fibroblasts with collagen I increases secretion of procathepsin B. J Biol Chem. 2002; 277:32220–7. [PubMed: 12072442]

33. Kuperwasser C, Chavarria T, Wu M, Magrane G, Gray JW, Carey L, et al. Reconstruction of functionally normal and malignant human breast tissues in mice. Proc Natl Acad Sci U S A. 2004; 101:4966–71. [PubMed: 15051869]
34. Sameni M, Anbalagan A, Olive MB, Moin K, Mattingly RR, Sloane BF. MAME models for 4D live-cell imaging of tumor: microenvironment interactions that impact malignant progression. J Vis Exp. 2012 pii:3661.
35. Mullins SR, Sameni M, Blum G, Bogyo M, Sloane BF, Moin K. Three-dimensional cultures modeling premalignant progression of human breast epithelial cells: role of cysteine cathepsins. Biol Chem. 2012; 393:1405–16. [PubMed: 23667900]
36. Laajala TD, Corander J, Saarinen NM, Makela K, Savolainen S, Suominen MI, et al. Improved statistical modeling of tumor growth and treatment effect in preclinical animal studies with highly heterogeneous responses in vivo. Clin Cancer Res. 2012; 18:4385–96. [PubMed: 22745104]
37. Weigelt B, Ghajar CM, Bissell MJ. The need for complex 3D culture models to unravel novel pathways and identify accurate biomarkers in breast cancer. Adv Drug Deliv Rev. 2014; 69–70:42–51.
38. Debnath J, Brugge JS. Modelling glandular epithelial cancers in three-dimensional cultures. Nat Rev Cancer. 2005; 5:675–88. [PubMed: 16148884]
39. Rothberg JM, Bailey KM, Wojtkowiak JW, Ben-Nun Y, Bogyo M, Weber E, et al. Acid-mediated tumor proteolysis: contribution of cysteine cathepsins. Neoplasia. 2013; 15:1125–37. [PubMed: 24204192]
40. Rixe O, Fojo T. Is cell death a critical end point for anticancer therapies or is cytostasis sufficient? Clin Cancer Res. 2007; 13:7280–7. [PubMed: 18094408]
41. Finak G, Bertos N, Pepin F, Sadekova S, Souleimanova M, Zhao H, et al. Stromal gene expression predicts clinical outcome in breast cancer. Nat Med. 2008; 14:518–27. [PubMed: 18438415]
42. Farmer P, Bonnefoi H, Anderle P, Cameron D, Wirapati P, Becette V, et al. A stroma-related gene signature predicts resistance to neoadjuvant chemotherapy in breast cancer. Nat Med. 2009; 15:68–74. [PubMed: 19122658]
43. Garber K. MET inhibitors start on road to recovery. Nat Rev Drug Discov. 2014; 13:563–5. [PubMed: 25082276]
44. Spigel DR, Ervin TJ, Ramlau R, Daniel DB, Goldschmidt JH, Blumenschein GR, et al. Final efficacy results from OAM4558g, a randomized phase II study evaluating MetMAb or placebo in combination with erlotinib in advanced NSCLC. J Clin Oncol Abstr. 2011; 29:7505.
45. Pennacchietti S, Michieli P, Galluzzo M, Mazzone M, Giordano S, Comoglio PM. Hypoxia promotes invasive growth by transcriptional activation of the met protooncogene. Cancer Cell. 2003; 3:347–61. [PubMed: 12726861]
46. Chen HH, Su WC, Lin PW, Guo HR, Lee WY. Hypoxia-inducible factor-1alpha correlates with MET and metastasis in node-negative breast cancer. Breast Cancer Res Treat. 2007; 103:167–75. [PubMed: 17028975]
47. Wilson WR, Hay MP. Targeting hypoxia in cancer therapy. Nat Rev. 2011; 11:393–410.
48. Sheridan C. Genentech to salvage anti-MET antibody with subgroup analysis. Nat Biotech. 2014; 32:399–400.

Translational Relevance

There is a critical need for effective targeted therapies for triple-negative breast cancer (TNBC) patients. The evaluation of treatment strategies is challenged by the intertumoral heterogeneity within TNBC and its surrounding tumor microenvironment (TME). The receptor tyrosine kinase MET is highly expressed in several TNBC subtypes and is a promising therapeutic target. In this study, we utilized unique *in vitro* and *in vivo* preclinical models that recapitulate the breast cancer TME and paracrine signaling factors. Using the inhibitor cabozantinib (XL184), we evaluated the efficacy of MET inhibition on 3D TNBC growth and invasion over time. We observed that cabozantinib significantly inhibited TNBC growth and invasion of diverse TNBC cell lines, yet was ineffective against MET^{neg} TNBC cells. *In vivo*, cabozantinib blocked TNBC tumor growth and metastasis in $hHGF^{tg}$-SCID mice. These results demonstrate that cabozantinib inhibition may be a highly effective treatment strategy for TNBC patients.

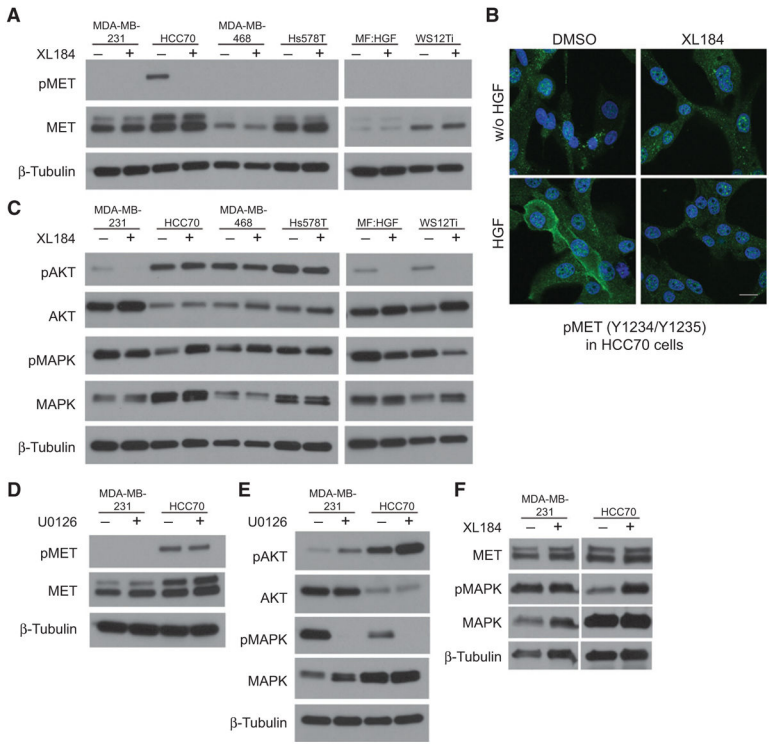

Figure 1.

XL184 has distinct effects on MET, AKT, and MAPK signaling in human TNBC cells and breast fibroblasts. Immunoblot analysis was used to evaluate the effect of XL184 treatment on 2D and 3D monocultures of TNBC cells and fibroblasts. A, analysis of monocultures revealed that MET is highly expressed but not constitutively active in diverse TNBC cell lines, not expressed in MF:HGF cells, and weakly expressed in Ws12Ti CAFs. B, confocal immunofluorescence analysis of pMET (Y1234/Y1235) in HCC70 cells that were untreated (DMSO), XL184-treated (2 μmol/L), HGF-treated (100 ng/mL), and XL184 + HGF treated. Blue pseudocolor, DAPI nuclear stain. Scale, 20 μm. C, AKT and MAPK signaling was differentially effected by XL184 treatment in TNBC cell lines and fibroblasts. D, MEK inhibition with 10 μmol/L U0126 had no effect on MET expression or activation in TNBC monocultures (E), but resulted in increased AKT phosphorylation and loss of MAPK activity. F, inhibition of MET in 3D monocultures caused similar changes in MAPK activity as compared with what was observed in 2D monocultures. β-Tubulin was used as a loading control.

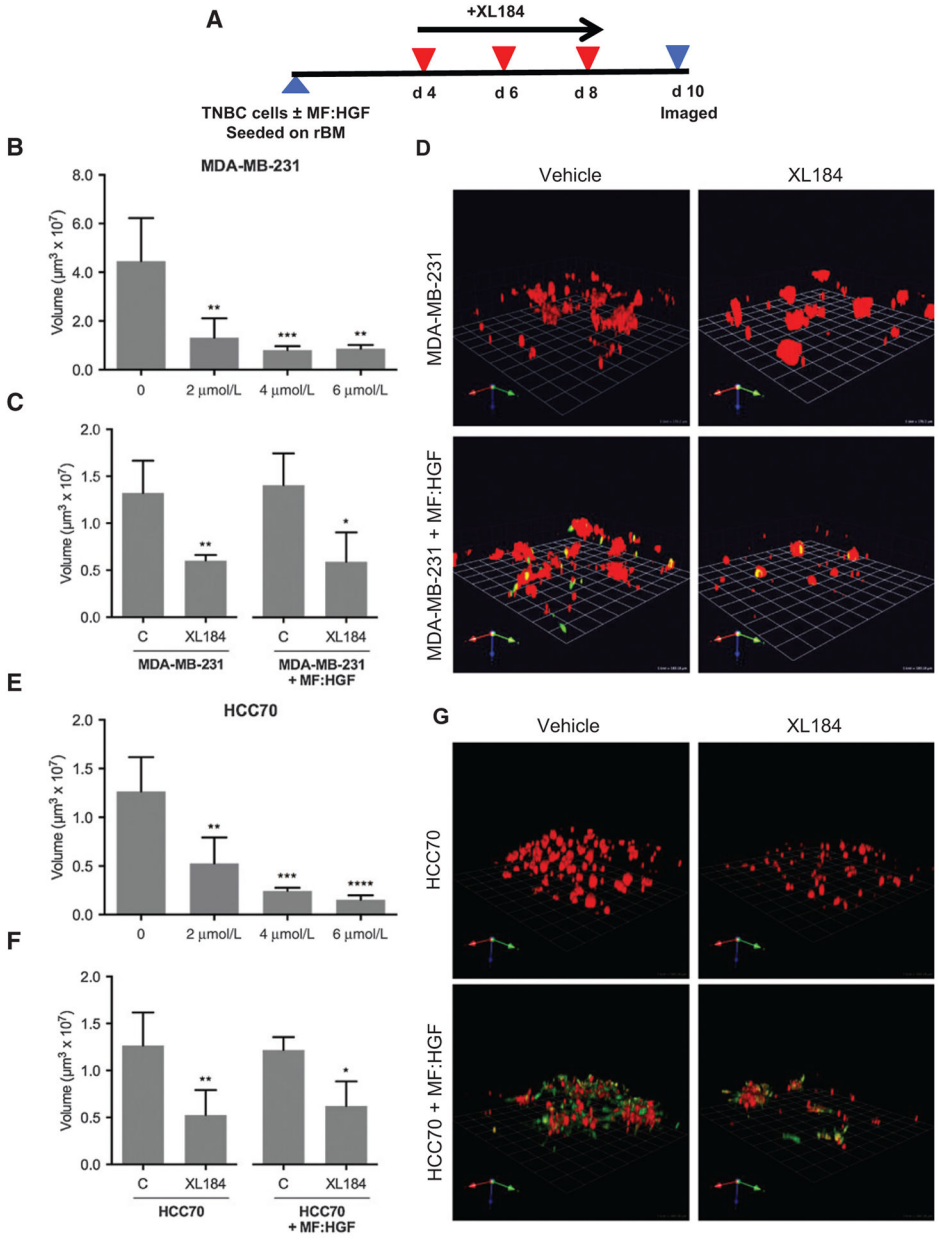

Figure 2.

XL184 reduces TNBC structures. A, experimental time course started with seeding TNBC cells in 3D rBM overlay cultures with or without fibroblasts. Vehicle control or XL184 was added at day 4, replaced every 2 days, and structures were imaged on day 10. B, XL184 significantly reduced the volume of MDA-MB-231 structures at 2 to 6 µmol/L. C, XL184 treatment significantly reduced the volume of both MDA-MB-231 monocultures and cocultures with MF:HGF cells. D, representative 3D reconstructions illustrate volume and number of MDA-MB-231 (red) structures in both monocultures and cocultures with MF:HGF cells (green). E, XL184 significantly reduced the volume of HCC70 structures at 2 to 6 µmol/L. F, XL184 treatment significantly reduced the volume of both HCC70

monocultures and cocultures with MF:HGF cells. G, representative 3D reconstructions illustrate volume and number of HCC70 (red) structures in both monocultures and cocultures with MF:HGF cells (green). Volumes were quantified in 64 fields (16 contiguous fields/experiment) from four independent experiments (one grid unit, 180 μm) and *P* values were calculated by Student *t* test (*, $P < 0.05$; **, $P < 0.01$; ***, $P < 0.0001$).

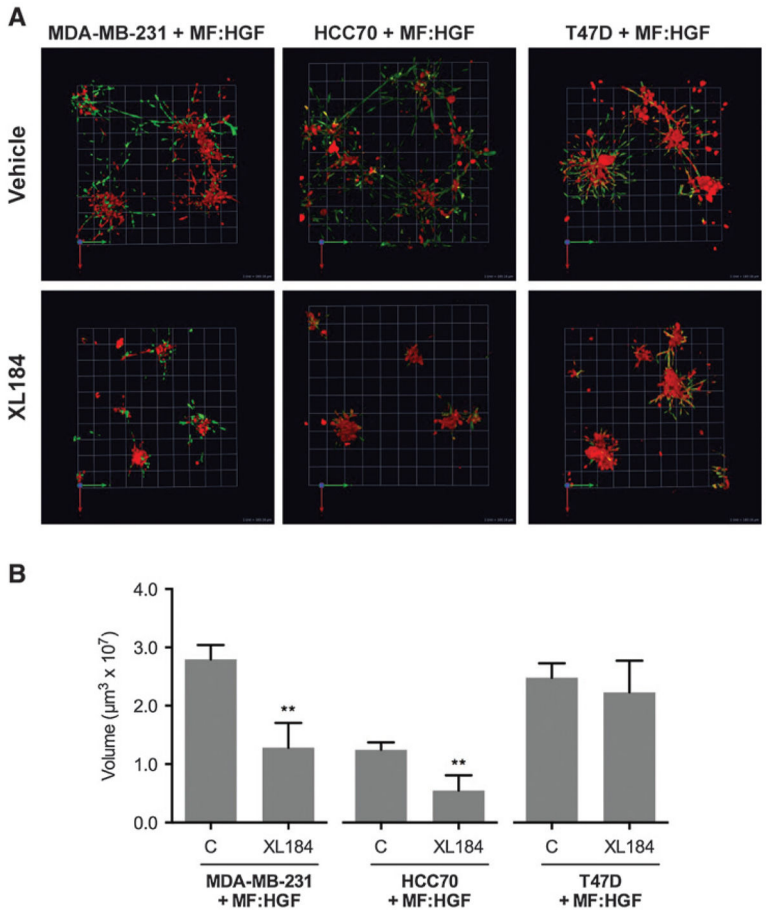

Figure 3.

XL184 has no effect on invasion or volume of MET^{neg} TNBC cells. Cocultures were treated with 2 μmol/L XL184 and imaged and analyzed as described in Fig. 2. A, XL184 treatment reduces invasive phenotype of MET^{pos} MDA-MB-231 and HCC70 cell:fibroblast structures, but not MET^{neg} T47D cell: fibroblast structures as illustrated by representative en face views of 3D reconstructions. B, structures formed by MET^{pos} MDA-MB-231 and HCC70 cells in coculture with fibroblasts exhibited a significant reduction in volume with XL184 treatment, whereas those formed by MET^{neg} T47D cells in coculture with fibroblasts were not significantly reduced in volume ($P > 0.4$) with XL184 treatment. Effects of XL184 treatment were quantified in 64 fields as described in Fig. 2 legend. Data are shown as the mean ± SD of three independent experiments and the Student *t* test was used to evaluate significance (**, $P < 0.01$).

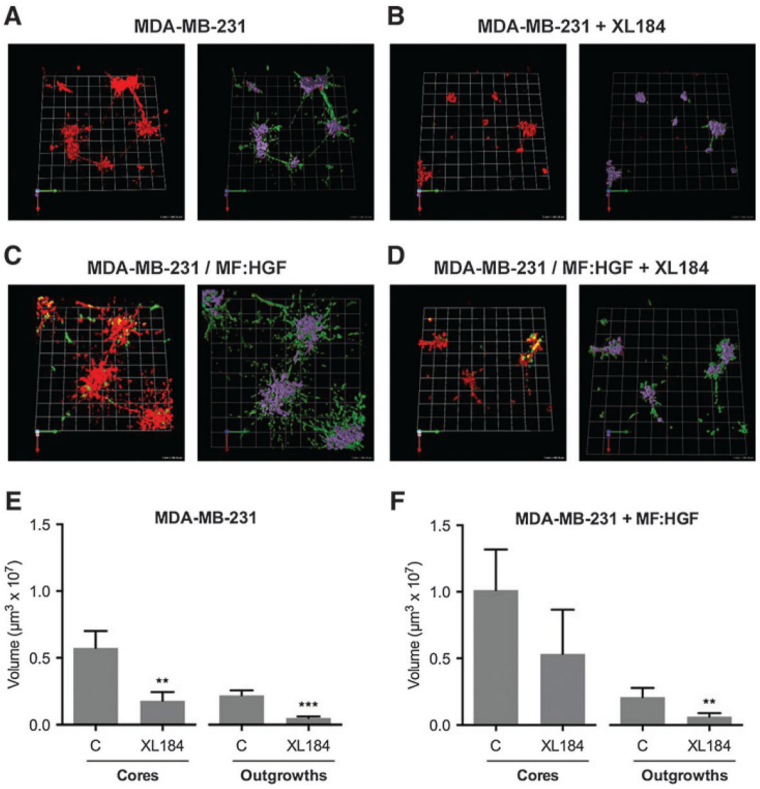

Figure 4.

XL184 significantly reduces volume of multicellular outgrowths from TNBC structures. A, vehicle control: 3D reconstructions of MDA-MD-231 structures (red, left) and segmentation using Volocity software into central cores (purple) and invasive outgrowths (green, right). B, XL184 treatment: 3D reconstructions of MDA-MD-231 structures (red) treated with XL184 (left) and segmentation into central cores (purple) and invasive outgrowths (green, right). C, vehicle control: 3D reconstructions of MDA-MB-231 structures (red) interacting with MF: HGF cells (green, left) and segmentation into central cores (purple) and invasive outgrowths (green, right). D, XL184 treatment: 3D reconstructions of MDA-MB-231 structures (red) interacting with MF: HGF cells (green, left) and segmentation into central cores (purple) and invasive outgrowths (green, right). XL184, added at time of seeding, reduced volumes in 6-day cultures of both cores and invasive outgrowths of structures formed by MDA-MB-231 cells alone (E) and reduced volume of invasive outgrowths of structures formed by MDA-MB-231 and MF:HGF co-cultures (F). Data are shown as the mean ± SD of four independent experiments (64 fields) and the Student *t* test was used to evaluate significance (**, $P < 0.01$; ***, $P < 0.0001$).

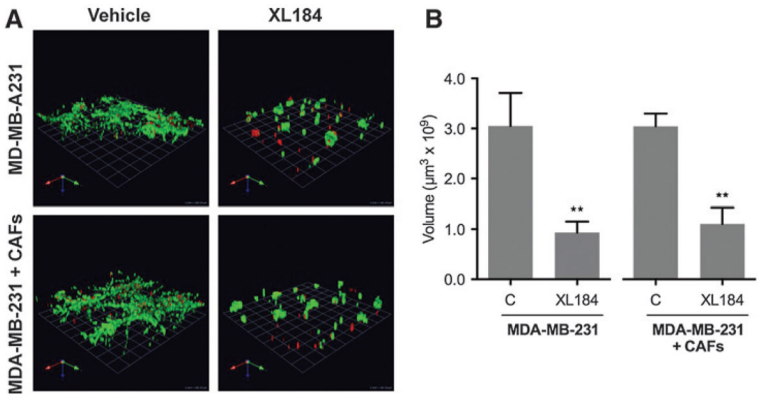

Figure 5.

XL184 treatment reduces the number and volume of live TNBC structures. TNBC cells were seeded in 3D reconstituted basement membrane overlay cultures alone or with human breast CAFs as described in Fig. 2 and treated with 2 μmol/L XL184 every other day. Viability was determined by a Live/Dead assay on day 12. A, representative 3D reconstructions of Live/Dead assays of MDA-MB-231 or MDA-MB-231 + CAF structures illustrating reduction in number of viable (green) TNBC cells. B, XL184 treatment significantly reduced the volume of live TNBC cells alone and in coculture with CAFs as quantified in 48 fields (16 fields/experiment and three independent experiments). Statistical significance was determined by the Student *t* test (**, $P < 0.01$).

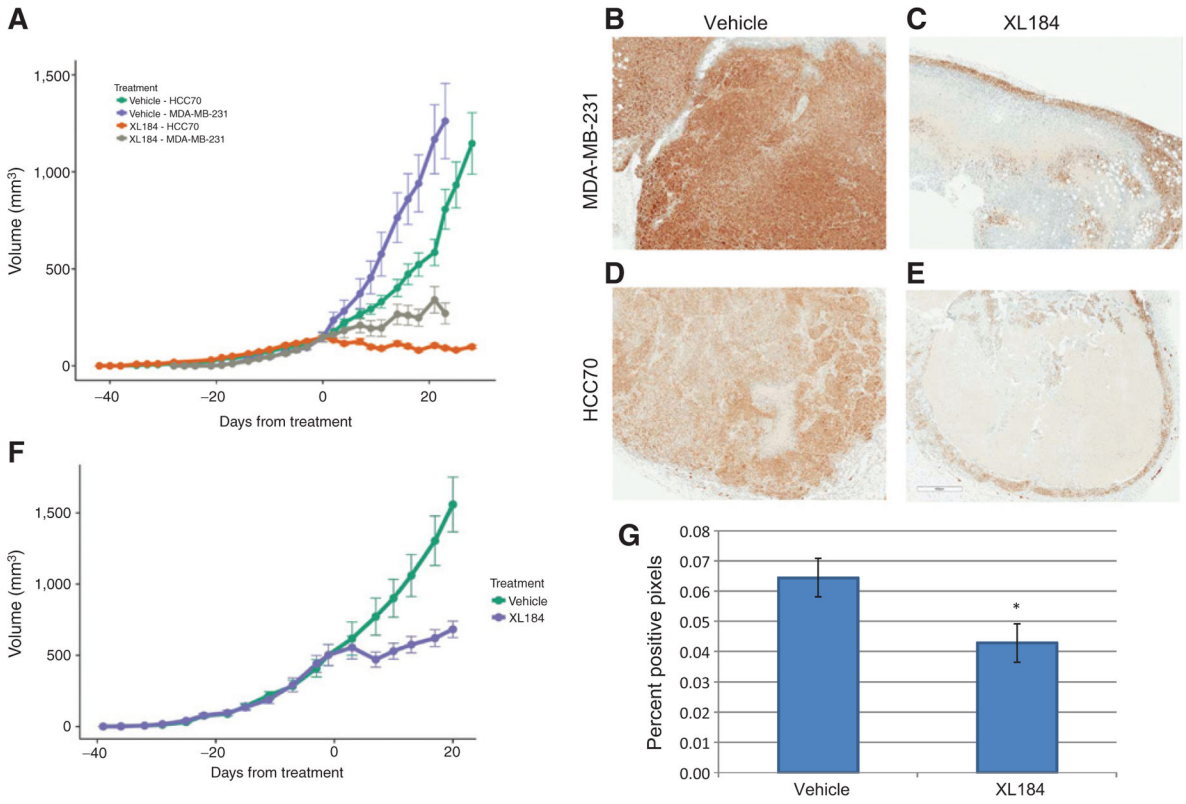

Figure 6.

XL184 treatment inhibits TNBC tumor growth and lung metastases *in vivo*. A, growth of orthotopic MDA-MB-231 and HCC70 tumors in hHGF^{tg}-SCID mice was significantly inhibited by 30 mg/kg XL184 treatment (MDA-MB-231, $P < 0.015$; HCC70 $P < 0.001$). B to E, pMET immunostaining was performed on MDA-MB-231 and HCC70 tumors treated with XL184 or vehicle (×40 magnification). F, established MDA-MB-231 tumors were significantly inhibited by 30 mg/kg XL184 treatment ($P < 0.005$). Linear mixed-effects modeling was used to test for significant differences in tumor growth. G, lung metastasis of MDA-MB-231 cells was significantly inhibited by treatment with 30 mg/kg XL184. Statistical significance was determined by the Student *t* test (*, $P < 0.02$) and data are shown as mean ± SE.